ELSEVIER

Journal of Chromatography A, 841 (1999) 75–94

JOURNAL OF CHROMATOGRAPHY A

Optimization of large-volume on-column injection conditions in gas chromatography by monitoring the actual carrier gas flow

Thomas Hankemeier*[,1], Sander J. Kok, René J.J. Vreuls, Udo A.Th. Brinkman

Free University, Department of Analytical Chemistry, De Boelelaan 1083, 1081 HV Amsterdam, The Netherlands

Received 21 September 1998; received in revised form 4 February 1999; accepted 5 February 1999

Abstract

The change of the evaporation rate of the solvent during injection and evaporation is the most critical aspect during optimization of large-volume on-column injection conditions in gas chromatography. The change is caused by the pressure drop along the retention gap when using an early solvent vapour exit (SVE) and can be described by a mathematical model. Four procedures for the optimization of the injection conditions were compared. It was found that different procedures often yield different evaporation rates, which may also depend on the injection speeds used during optimization. For optimization of a new set-up, i.e. if little is known about the optimal injection conditions, the evaporation rate should be determined by increasing the injection time at a fixed injection speed, injection temperature and head pressure; subsequently, an appropriate injection speed can be calculated. If a mere re-optimization is required as e.g. after the exchange of the retention gap, adjusting the evaporation rate to the injection speed by varying the injection temperature at a constant injection speed is the preferred procedure. With both methods, optimization can be achieved by means of 2–5 injections of pure solvent and monitoring the helium carrier gas flow. That is, optimization of the injection conditions takes less than 1 h. When using this strategy, analytes as volatile as monochlorobenzene can be determined in aqueous samples by in-vial liquid–liquid extraction–gas chromatography–mass spectrometry. Closing the SVE at the very end of solvent evaporation results in a considerable increase of the capacity of the retention gap compared to closing the SVE before all solvent is evaporated.

Keywords: Large-volume injections; Solvent vapour exit; Mathematical modelling; Evaporation rate; Automation

1. Introduction

1.1. Large-volume on-column injection and aim of the study

Today, large-volume injections, i.e. the injection of volumes larger than 1–5 μl, are increasingly used in gas chromatography (GC) to improve analyte detectability (in concentration units) [1–3]. This approach also allows the use of new strategies in sample preparation [4]. To quote an example, the injection of a larger aliquot of an extract makes in-vial liquid–liquid extraction (LLE) much more attractive, because the sample volume can be decreased from 100–1000 ml to 1–10 ml [5].

On-column injection is the preferred technique for the introduction of up to 250 μl of sample if the

*Corresponding author. Tel.: +31-20-4447525; fax: +31-20-4447543.

[1]Present address: TNO Insitute for Nutrition and Food Research, Analytical Sciences Division, Utrechtseweg 48, 3704 HE Zeist, The Netherlands. Tel.: +31-30-6944297.

0021-9673/99/$ – see front matter
PII: S0021-9673(99)00201-0

determination of volatile analytes is the main goal and the sample extract is not too contaminated. The solvent is injected into a retention gap, which is connected to a retaining precolumn or, directly, to the analytical column. For the on-column injection of larger volumes, two parameters have to be carefully chosen. (1) An early solvent vapour exit (SVE) is generally inserted between the retaining precolumn and the analytical column to allow faster evaporation and to protect the detector from the solvent vapour. The SVE has to be closed at an appropriate moment in time [6]. (2) If a considerable part of the solvent evaporates during injection, so-called injection under partially concurrent solvent evaporation (PCSE) conditions [7], the injection speed has to be chosen to be larger than the evaporation rate to ensure the formation of a solvent film in the retention gap so that volatile analytes will be trapped without, however, the solvent film reaching the end of the retention gap [8].

1.1.1. SVE closure

Usually, the SVE is closed at a predetermined time just before the last drops of solvent evaporate, in order not to lose the volatile analytes. This moment in time is usually determined by monitoring the effluent leaving the SVE by a flame or by performing a series of injections at different closure times (viz. by determining when losses of the volatile analytes start to occur) [9,10]. Recently, we demonstrated that monitoring the helium flow into a GC by means of an electronic flow meter can be used to register the end of the evaporation process and effect the automated closure of the SVE [11]. During the injection and evaporation process the helium flow-rate decreases, mainly because of the presence of solvent vapour in the gas phase, and the completion of the evaporation process is indicated by a steep increase of the helium flow to its original value. Our approach makes optimization of a fixed point in time for the SVE closure superfluous. The system also becomes more robust: even when the evaporation time varies due to small changes of the injection speed or volume, closure of the SVE occurs just in time without loss of volatiles or a significant change of the solvent peak width in the detector.

1.1.2. Procedures for optimization of injection speed

There are two types of strategies to find the appropriate PCSE on-column injection conditions, viz. by means of injections of standard solutions of, e.g., *n*-alkanes or pure solvent. With the former approach, the injection speed is stepwise increased until solvent trapping causes reconcentration of the volatile analytes [10]. The set-up does not have to be changed, but the optimization procedure can take up to one day, even for an experienced analyst. We therefore focused on strategies which use injections of pure solvent and determination of the evaporation time to reduce the time required for optimization.

With all of the proposed methods A–C (which are described in Section 1.2), the evaporation time can be determined from the solvent peak width registered with a flame ionization detector (modification of the set-up required) or a flame or, more precisely ([11]), by the (automated) monitoring of the helium flow. It is, also, tacitly assumed that the evaporation rate is independent of the injection speed. However, recently we demonstrated that this is not true. The dependence of the evaporation rate on the injection speed could be attributed to a pressure drop along the length of the retention gap and the restriction of the gas flow by the formation of a solvent film within the retention gap [11]. Recently, this phenomenon was also reported by Boselli et al. [12]. This makes evaporation rates as were calculated by Staniewski and Alejski [13], who did not consider the influence of the solvent film, somewhat unreliable.

1.1.3. Aim of the study

In the present paper, critical aspects of the optimization of the conditions for large-volume on-column injection are discussed. Monitoring of the helium carrier gas flow was used to study the influence of the moment of SVE closure on the length of the flooded zone and the role of inserting and withdrawing the injection needle on the evaporation rate. A mathematical model was developed to help interpret the change of the evaporation rate during injection and to study the influence of this phenomenon on the determination of the evaporation rate by means of methods A–C. The aim was to find an efficient strategy for the optimization of the injection con-

ditions by (automated) monitoring of the carrier gas flow. The practicality of the new approach was demonstrated by the determination of volatile microcontaminants in water by in-vial LLE–GC–MS.

1.2. Procedures for optimization of injection speed

Three procedures are based on the determination of the evaporation rate and subsequent calculation of an appropriate injections speed (methods A1, A2 and B, see below). When the evaporation rate, ν_{evap} (μl/min), the length of the retention gap, L_{RG} (cm), and the flooded zone, FZ (cm/μl), are known, one can calculate the injection speed, ν_{inj} (μl/min) at which a certain length of the solvent film in the retention gap (expressed as the fraction, *f*, of the total length of the retention gap) for a given sample volume, V_{inj} (μl), is obtained, from (see [9,14]):

$$\nu_{inj} = \frac{\nu_{evap}}{1 - \frac{f \times L_{RG}}{V_{inj} \times FZ}} \quad \text{(I)}$$

1.2.1. Method A

One option is to determine the evaporation rate by increasing the injection speed at a constant injection time and head pressure, and plotting the evaporation time vs. the injection volume. As is depicted in Fig. 1 below, the evaporation rate then equals the injection speed at the point of intersection of the two parts of the plot (method A1). Alternatively, the evaporation rate can be calculated from the slope of the high-injection speed part of the same plot, because it is equal to the inverse of that slope expressed as (Δ evaporation time/Δ injection volume) [9, p. 255] (method A2).

1.2.2. Method B

As an alternative, the evaporation rate can be calculated from the slope of a plot of evaporation time vs. injection time, recorded at constant injection speed, where the evaporation rate again equals the inverse of the slope expressed as (Δ evaporation time/Δ injection volume). Obviously, the evaporation time has to be longer than the injection time, as otherwise injections will be made under fully concurrent evaporation conditions and no significant amount of solvent will be left in the retention gap during injection.

1.2.3. Method C

If only slight changes of the set-up have to be made – that is, if the optimal injection conditions are rather well known – a simpler strategy can be used. In this case, the evaporation rate is varied by changing the injection temperature at a fixed injection speed and head pressure to adjust the evaporation rate to the injection speed. The injection temperature is varied and the ratio (injection time/evaporation time), called ϑ, which is identical with the percentage of solvent evaporated during injection, is determined for the injection of pure solvent until a pre-selected target value is obtained (for details, see Section 3.4.2).

2. Experimental

2.1. Chemicals

Ethyl acetate and *n*-hexane (both analytical-reagent grade, J.T. Baker, Deventer, The Netherlands) were distilled before use. For the test analytes, which came from various sources and were all of analytical-reagent quality, one is referred to Table 6 below. For on-column injections and spiking purposes, stock solutions were diluted to 1 ng/μl. Spiking of water samples was done just prior to analysis. The samples were spiked in the autosampler vial prior to extraction.

2.2. Set-up of large-volume injection–GC system

The large-volume injection (LVI)–GC system consisted of a Carlo Erba Series 8000 gas chromatograph equipped with an on-column injector and an FID-80 (CE Instruments, Milan, Italy) flame ionization detection (FID) system or an MD 800 mass spectrometer (CE Instruments); for a figure of the set-up one is referred to [11]. A Model F101D-HA flow meter (Bronkhorst, Ruurlo, The Netherlands) was inserted between the pressure regulator and the on-column injector. A 3-m diphenyltetramethyldisilazane (DPTMDS)-deactivated retention gap (0.53

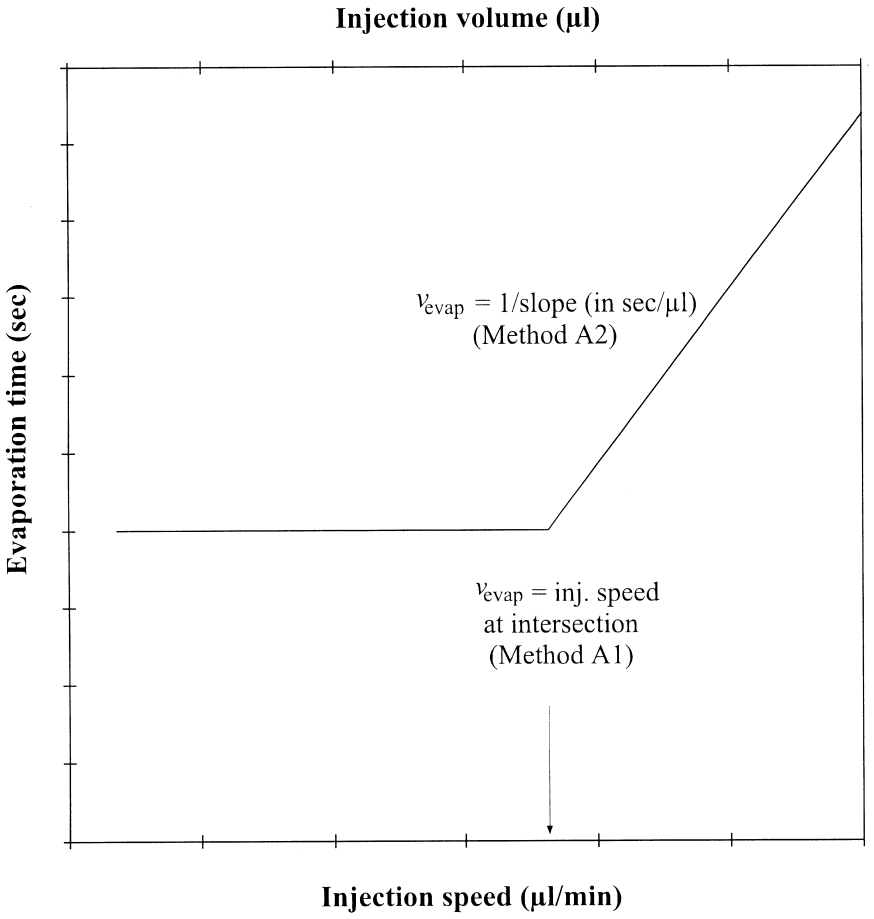

Fig. 1. Theoretical plot of evaporation time vs. injection speed and volume at a constant injection time, temperature and head pressure. The determination of the evaporation rate according to methods A1 and A2 is shown. The evaporation rate is assumed to be constant during injection and evaporation (for more details, see text).

mm I.D.; BGB Analytik, Zurich, Switzerland) was connected to a 2-m retaining precolumn and an 28-m analytical column (both DB-XLB, 0.25 mm I.D., film thickness 0.25 µm; J&W, Folsom, CA, USA) via a press-fit connector and a T-piece, respectively. The SVE, an electronically controlled 6-port valve (Valco Instruments, Houston, TX, USA), was connected to the T-piece and was controlled by the SVE controller [11; also see below]. Helium 5.0 (Hoekloos, Schiedam, The Netherlands) was the carrier gas. If not otherwise stated, the standard boiling point of a solvent was used as initial GC temperature, i.e. 77°C for ethyl acetate and 69°C for *n*-hexane, and the head pressure was 100 kPa.

For injections with an automated syringe pump (Harvard Apparatus 22, So. Natick, MA, USA), a 500-µl syringe with a PTFE-coated plunger was used. After filling and mounting it in the Harvard pump, the sample was transferred to the on-column injector via a stainless steel needle (O.D. 0.25 mm).

For LLE–LVI-GC–MS of aqueous samples, an AS 800 autosampler (CE Instruments) and a 250-µl syringe with PTFE plunger and an injection needle of 0.5 mm O.D. were used. The proper settings for the autosampler were programmed by means of CHROMCARD Ver. 1.33 (Fisons Instruments, Manchester, UK) for FID, and on the controller of the autosampler in the case of MS detection.

After optimization had been achieved and sample analyses were being performed, the injection needle

was removed 0.05 min after completion of the injection (during optimization the needle was removed only after the end of the evaporation).

After the automated closure of the SVE by the controller, the temperature programme of the GC system was started after a delay of 2 min. The temperature was increased to 280°C at 10°C/min, and held at 280°C for 5 min.

2.3. FID monitoring of solvent peak

Next to the carrier gas flow-rate profile, the solvent peak was monitored, viz. with FID. A press-fit splitter was connected to the retention gap. A 0.6 m×0.05 mm I.D. fused-silica restriction was used to direct about 0.04% of the gas flow to the FID system. The other outlet of the T-splitter was connected to 0.3–0.5 m of a 0.32 mm I.D. retention gap. In order to record the whole solvent peak, the air flow of the FID system was increased to 1500 ml/min by removing the restriction in front of the pressure controller, and the range was set to 10^3.

2.4. Automated detection of end of evaporation and SVE closure

A laboratory-made and microprocessor-based SVE controller with a small keyboard and LCD display was constructed to actuate the closure of the SVE. As soon as the first derivative of the helium flow exceeded a pre-set threshold value, the SVE was closed and the GC run started. All relevant parameters, i.e. the threshold value and delay times could be programmed in this controller and were stored in its memory. The closure times of the SVE were stored in the memory of the SVE controller and could be displayed for 50 injections (for more details, see [11]).

When ready for a next run, the GC instrument gave a start signal to the AS 800 autosampler. When the autosampler was ready for injection, a signal was given to the SVE controller to open the SVE. After a delay of 0.05 min, the injection was started. The syringe was removed. After an additional delay of 0.05 min to allow stabilization of the helium flow, monitoring of the helium flow by the SVE controller was initiated.

2.5. Determination of flooded zones

The flooded zone was determined by injecting a 1 ng/μl (experiments with SVE closed during injection) or 0.2 ng/μl (experiments with SVE open during injection) solution of *n*-alkanes in ethyl acetate, and recording at which injected volume prepeaks due to flooding of the retaining precolumn started to occur. The head pressure was 115 kPa and the helium flow 12.5 ml/min (SVE open) or 1.5 ml/min (SVE closed). With the SVE open, the evaporation rate was found to be 45 μl/min. Injections with the SVE closed during injection were done with the AS 800 autosampler at a speed of 120 μl/min (injection volumes for SVE closed also during evaporation: 10–22 μl; for SVE open during evaporation: 30–70 μl). For experiments with the SVE open during injection, injection was done with the Harvard pump at 71 μl/min (injection volumes: 118–178 μl).

3. Results and discussion

3.1. Influence of injection needle diameter

When the original injection syringe of the AS 800 autosampler with an O.D. of 0.5 mm was inserted into the on-column injector, the helium flow decreased ≈12% at a head pressure of 50 kPa due to the increased resistance in the gas-flow system (Fig. 2, all traces). At the start of the injection, the helium flow-rate sharply decreased, as is evident from traces B and C; with trace A no injection was made. If the syringe was removed at the end of the injection (traces A and B), the helium flow increased again. The end of the evaporation process was indicated by another, sharp, increase of the helium flow-rate, which is the basis of our current procedure of automated closure (traces B and C). The time required for the evaporation of the solvent left in the retention gap was less if the syringe was removed at the end of the injection (trace B) than when it was not removed (trace C). This can be attributed to elimination of the pressure drop along the length of the injection needle in the retention gap upon removal of the needle and, consequently, in an increase of the evaporation rate.

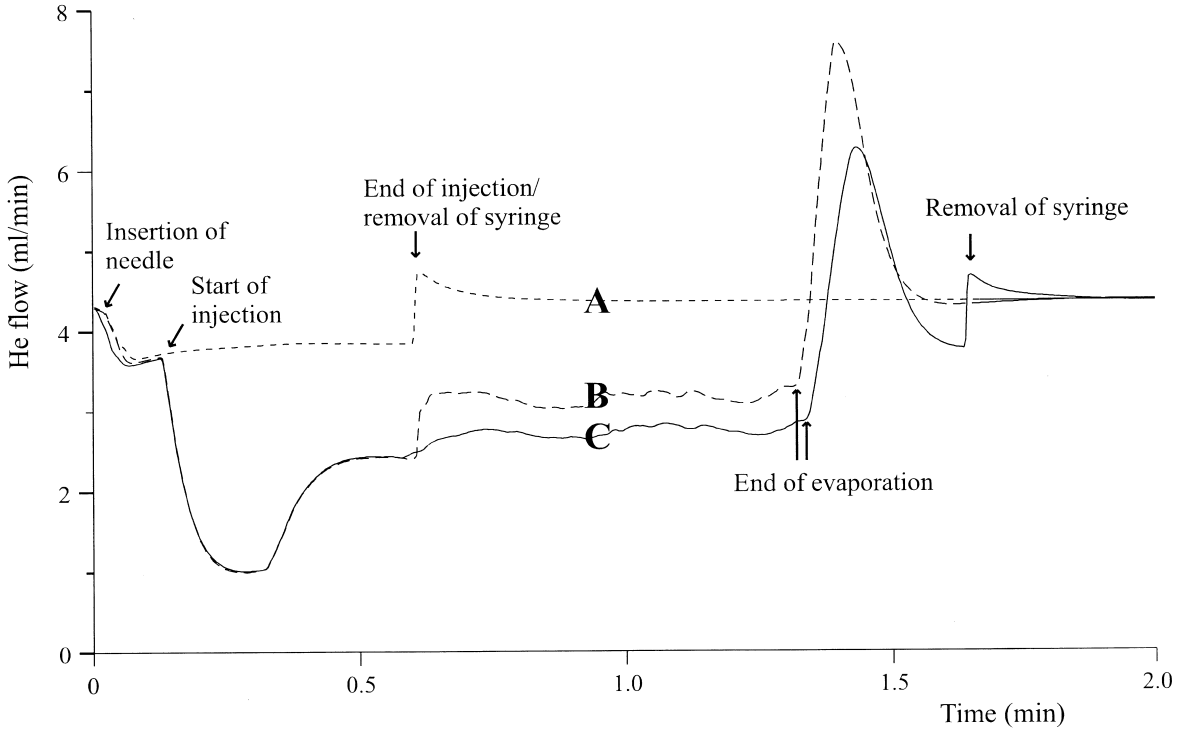

Fig. 2. Helium flow-rate profile for (A) inserting and withdrawing of needle without injection, and (B and C) a 30-μl injection of ethyl acetate with SVE open and with (B) and without (C) removing the injection needle at the end of the injection. Injection speed, 60 μl/min; head pressure, 50 kPa; for further details, see text.

When using a custom-made injection needle of 0.25 instead of 0.5 mm O.D., the helium flow decreased only about 1% upon needle insertion, and there was no noticeable change of the evaporation rate or time upon needle insertion/removal.

3.2. Dependence of flooded-zone length on SVE closure time

The solvent film formed during injection is slowly pushed further into the retention gap by the carrier gas flow after the injection is complete and, the longer the solvent evaporation takes, the further will the film extend into the retention gap [9,15]. That is, the longer evaporation takes, the longer will be the flooded zone, and the less solvent will fit in the retention gap without flooding the retaining pre-column or, in other words, the smaller will be the 'capacity' of the retention gap. When studying the dependence of the flooded-zone length on the closure time of the SVE, one should consider that, if the determination of volatile analytes is the goal, the SVE should be closed before the last drop of liquid disappears [6]. This implies that, in practice, one closes the SVE somewhat too early to be on the safe side.

The influence of the time of SVE closure on the flooded zone of a 3.1 m×0.53 mm I.D. DPTMDS-deactivated retention gap was determined for three sets of conditions: (1) the SVE was kept closed during injection and evaporation, (2) the SVE was open during injection and closed just when evaporation was complete, and (3) the SVE was opened only at the end of the injection and closed just when evaporation was complete. Closure was initiated by the SVE controller.

When the SVE was kept closed, the flooded zone was found to be 15.5 cm/μl. However, when the SVE was open after the injection, i.e. during the final part of the evaporation, the flooded zones were much

smaller, viz. 6.0 cm/μl (SVE open at end of injection) and 5.6 cm/μl (SVE open during injection and evaporation). The large differences illustrate the major influence of having the SVE open after completion of the injection and not closing the SVE too early.

The flooded zones reported in the recent literature for injections with the SVE open during injection, but (probably) being closed before evaporation was complete, are in between the values of ≈6 and ≈15 cm/μl found by us. Vreuls et al. reported a flooded zone of 10 cm/μl for ethyl acetate into a DPTMDS-deactivated retention gap of 0.53 mm I.D at an injection temperature of 83°C [16]. Grob reported a flooded zone of about 11 cm/μl for a wetted and uncoated retention gap of 0.53 mm I.D. if the injection temperature is less than 20°C below the pressure-corrected boiling point [9, p. 209]. Recently, Boselli et al. reported flooded zones of about 3 cm/μl for large-volume injections into a 0.53 mm I.D. retention gap [12].

Obviously, closing the SVE just in time causes a considerable reduction of the flooded zone and thereby maximizes the capacity of the retention gap. This will allow a considerable reduction of the length of the retention gap or the injection of a larger volume, or it will provide a larger margin with regard to variations of e.g., the injection volume. Therefore, in the rest of the study, the SVE was always closed at the very end of the solvent evaporation.

3.3. Calculation of evaporation rate during injection and evaporation

The helium flow depends on three parameters, (1) the ratio of the vapour pressures of helium and the solvent used, (2) the viscosity of the gas mixture, and (3) the flow resistance of the system [11]. The helium flow can be calculated from:

$$F_{He} = y_{He}\,(600\,\pi\,r^4/16\,\eta_m L)\,[(p_i^2 - p_o^2)/p_o]\,[p_o/p_{ref}][T_{ref}/T] \quad \text{(II)}$$

and the evaporation rate of the solvent, ν_{evap}, from:

$$\nu_{evap} = 1000\,[(1 - y_{He,\,exit})/y_{He,\,exit}]\,[M/(V_m d)]\,F_{He} \quad \text{(III)}$$

with: d, density of solvent (g/ml); F_{He}, flow-rate of helium (ml/min); η_m, viscosity of the helium and solvent gas mixture calculated according to Wilke's approximation (Poise) [13,17]; L, length of retention gap (cm); M, molecular mass of solvent (g/mol); p_i and p_o, pressures at inlet and outlet of the retention gap (Pa); p_{ref}, reference pressure, 1.013×10^5 Pa; r, internal radius of retention gap (cm); T, column temperature (K); T_{ref}, reference temperature, 298.15 K; evaporation rate of the solvent (μl/min); V_m, molar gas volume at T_{ref} and p_{ref} (101.3 kPa) (ml/mol); y_{He}, mole fraction of helium; $y_{He,\,exit}$, mole fraction of helium at exit of retention gap. The same assumptions were made as in the previous study, i.e. ideal gas behaviour of the solvent vapour and saturation of the gas phase with solvent vapour; a possible decrease of the retention gap temperature due to solvent evaporation was not considered. A pressure drop due to the insertion of the injection needle was accounted for by using a smaller internal diameter for that length of the retention gap in which the injection needle was inserted.

When injecting at a speed above the evaporation rate, ν_{evap}, the latter may change during the injection. The change itself will be dependent on the injection speed because of the pressure drop along the solvent film which causes a change of the ratio (helium pressure–solvent vapour pressure) and of the viscosity of the helium/solvent gas mixture. Eq. (II) is therefore valid for an infinitesimal part of the retention gap only, and the helium flow was calculated iteratively for a given moment in time [11]. The evaporation rate was calculated by incrementally increasing the time and calculating the actual solvent film distribution and the evaporation rate at that time. The (iterative) calculation was done by means of a programme written as visual basic macro and a spreadsheet programme as shown in Table 1.

It is possible to calculate the solvent vapour flow (expressed in μl liquid/min; Fig. 3, curves d and h) at any position in the retention gap at any moment in time by using the mole fraction of helium at that position rather than at the exit of the retention gap as in Eq. III (in the latter case, the evaporation rate is obtained). In Fig. 3 this is shown in the upper frame for the final moment of a 120-μl/min injection into a 5.95 m×0.32 mm I.D. retention gap. Whereas the solvent pressure is constant along the solvent film

Table 1
Programme used to calculate evaporation rate

No.	Step	Comment
1	Read variables	Variables read, e.g., head pressure, injection speed, injection time, length and I.D. of retention gap (RG), retaining precolumn and capillary to SVE
2	Calculate evaporation rate at start of injection ($t=0$)	Solvent film of 15-cm length is assumed for calculation of evaporation rate at start
3	Repeat until end of evaporation:	
	a: Increase time, t	t is iteratively increased by 0.02 min
	b: Calculation of amount of solvent in RG	$V_{s,t} = (v_{inj} - v_{evap,t-dt})*dt + V_{s,t-dt}$ with $V_{s,t}$, amount of solvent in RG at time t; dt, time increment; V_{inj}, injection speed $v_{evap,t-dt}$, evaporation rate at time $t-$dt.
	c: Check if evaporation is finished	If $V_{s,t} = 0$, then go to step 4.
	d: Calculation of solvent film	Solvent film distribution is an estimate, as it cannot be measured exactly. Calculation by algorithm during injection: solvent film thickness proportional to difference $v_{inj} - v_{evap,t}$, length dependent on $v_{inj} - v_{evap,t}$ and $V_{s,t}$. The (calculated) flooded zone depends on amount of solvent left in RG and solvent film length at end of injection. Position of last drop depends on injection speed, evaporation rate and volume injected. Flooded zones were (during injections of Table 2) 7.5–9.2 cm/μl for 0.32 mm I.D. and 3.6–4.8 cm/μl for 0.53 mm I.D. RGs. Film thicknesses were between 40 μm (at front end) and 10 μm (at end of evaporation) (for examples, see Fig. 2; details upon request from authors).
	e: Calculation of evaporation rate	For given solvent film distribution and helium flow, pressure profile along RG is calculated by iteratively increasing position along length of RG by means of Eq. (II), using mole fraction and viscosity from previous segment. Helium flow is iteratively increased until pressure at SVE exit is 101.3 kPa; evaporation rate calculated from Eq. (III).
	f: Write data to spreadsheet	
4	Calculate average evaporation rate, $v_{evap,\ average}$	$v_{evap,\ average} = (\Sigma_t v_{evap})/n$ with n, number of time increments
5	End of programme	

(Fig. 3, curve c), the solvent vapour flow increases along the length of the solvent film. This is primarily due to the (total) pressure drop (Fig. 3, curve a) along the retention gap and the resulting increase of the molar fraction of solvent in the gas phase (which is reflected by the increasing ratio (solvent pressure/helium pressure) of Fig 3, curve b). The further the solvent film reaches into the retention gap during the injection, the higher will the evaporation rate become. This effect is enhanced by the decrease of the viscosity connected with the higher mole fraction of the solvent vapour which has a lower viscosity than helium. This increase is only partly annulled by the increased restriction due to the presence of the

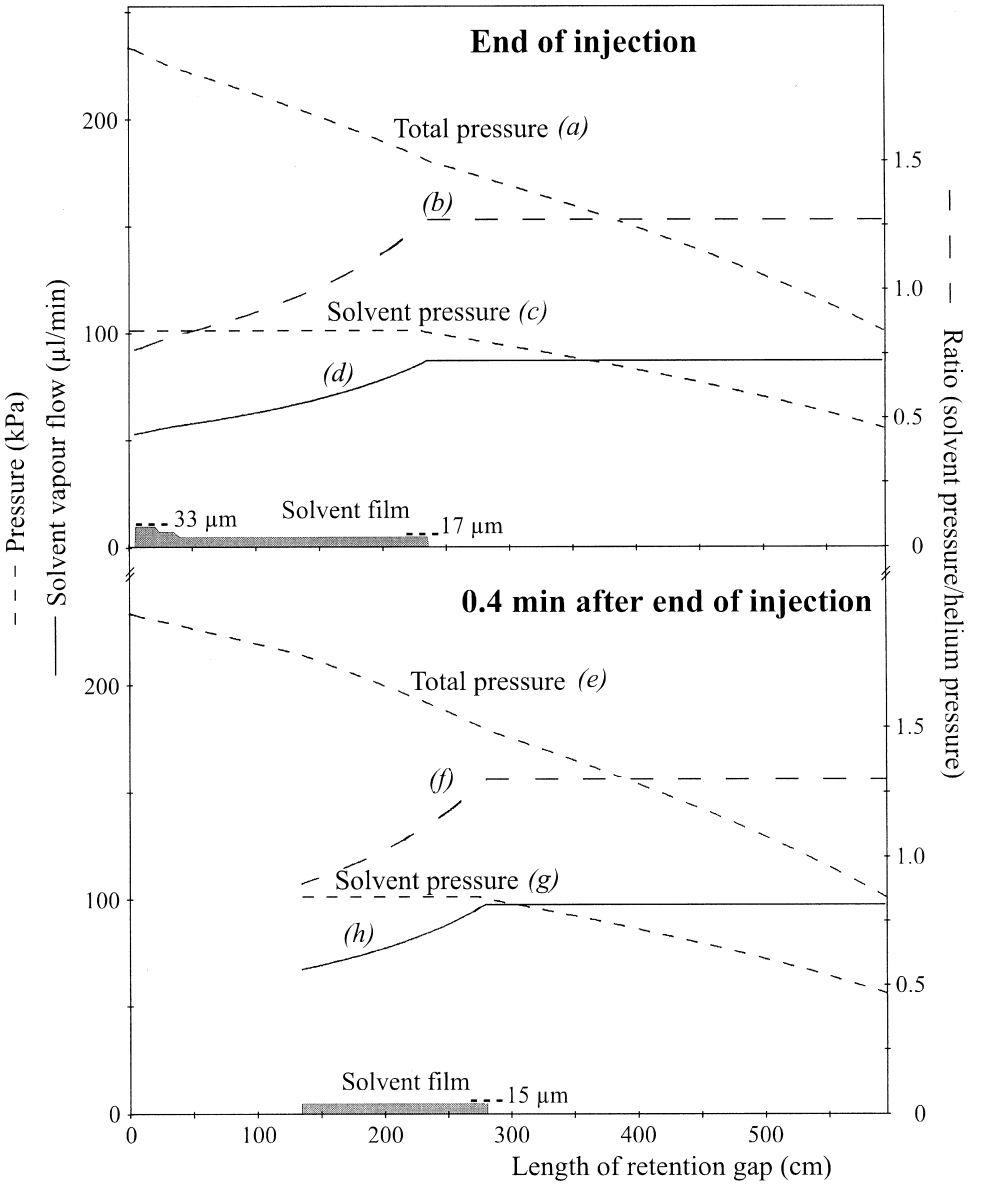

Fig. 3. Theoretical profiles of the solvent film distribution, the total pressure (a, e), the solvent pressure (c, g), the ratio (solvent pressure/helium pressure) (b, f) and the evaporation rate (d, h) for a 120-µl/min injection of ethyl acetate into a 5.95 m×0.32 mm I.D. retention gap at a head pressure of 132 kPa. Injection time, 1 min. The situation at the end of the injection (a–d) and 0.4 min after the end of the injection (e–h) are shown. The profiles were calculated by the programme of Table 1 and using Eqs. (II) and (III).

solvent film. This does not only result in evaporation at the rear end of the film, but also along the whole solvent film. After the injection, evaporation of solvent occurs (mainly) from the rear end of the solvent film, which therefore moves towards the end of the retention gap (Fig. 3, lower frame) until all of the solvent has evaporated. The evaporation rate increases as the rear end moves farther into the

retention gap, due to the smaller pressure drop along that part of the retention gap where there is no solvent film compared with the part with a solvent film (caused by the lower viscosity of pure helium) (Fig. 3, curve e).

3.3.1. Data for 0.32-mm I.D. retention gap

The change of the evaporation rate during injection was determined by splitting a small part of the eluting helium–solvent gas mixture via a restriction to an FID system. Relevant results are shown in Fig. 4 and Table 2. [Due to the dead time through the restriction of 0.04 min (solvent–helium mixture) up to 0.18 min (pure helium), start and end of injection and end of evaporation are recorded by FID with a delay of 0.04–0.18 min relative to the real time of the injection which is presented on the *x*-axis of Fig. 4.] To quote an example, as is to be expected from the above discussion, the experimentally observed increase of the evaporation rate of 18 μl/min (calculated with programme of Table 1: 12 μl/min) during the 120-μl/min injection into the 0.32 mm I.D. retention gap of set-up 1 (Table 2) is larger than that of 11 μl/min (calculated: 4 μl/min) for a 90-μl/min injection (Table 2 and Fig. 4). After the injection, the increase of the evaporation rate up to the end of the evaporation is 17 μl/min (calculated: 22 μl/min), which is larger than the 8 μl/min (calculated: 4 μl/min) of the 90-μl/min injection. Fig. 4 also shows that the evaporation rate increases more strongly after, than during, the injection.

3.3.2. Data for 0.53-mm I.D. retention gap

A similar trend in the evaporation rate is observed for injections into a 0.53 mm I.D.. However, the changes are less pronounced (see data of set-ups 2 and 3 of Table 2). To quote an example, for a 230- and a 320-μl/min injection into a 3.95 m×0.53 mm

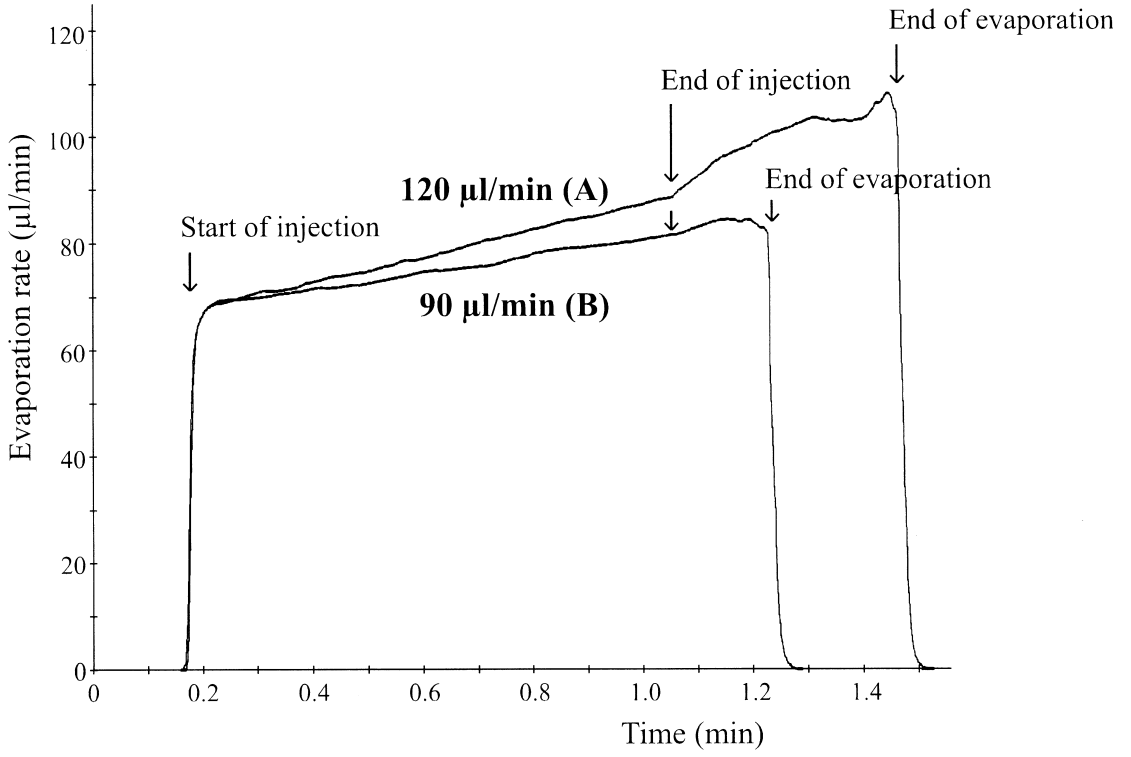

Fig. 4. Evaporation rate during 1-min injection of ethyl acetate at (A) 120 μl/min and (B) 90 μl/min into the 0.32 mm I.D. retention gap of set-up 1 of Table 2. The solvent peak was monitored with FID (for more details and the time *x* axis, see text). Head pressure, 132 kPa. The injection needle was not removed after the injection.

Table 2
Evaporation rate during large-volume on-column injections of ethyl acetate (calculated values in italics)

Set-up[a]				Solvent at end of injection[c] (μl)	Evaporation rate, experimental[b] or calculated (μl/min)			
No.	I.D. RG (mm)	P (kPa)	Injection speed (μl/min)		At start of injection[d]	At end of injection	At end of evaporation	Mean[e]
1	0.32	132	90	*14*	70	81	89	77
					75	*79*	*83*	*77*
			120	*41*	70	88	105	86
					75	*87*	*109*	*85*
2	0.53	25.2	250	*26*	–	–	–	197
					197	*190*	*231*	*201*
			350	*77*	–	–	–	212
					197	*207*	*318*	*219*
3	0.53	38.7	230	*21*	192	204	214	172
					187	*188*	*200*	*188*
			320	*67*	193	196	252	178
					187	*190*	*230*	*196*

[a] Set-up 1: 5.95 m×0.32 mm I.D. retention gap (RG); after 5.65 m T-splitter for 0.05 mm I.D. capillary to FID system; injection time, 1 min. Set-up 2: 4.85 m×0.53 mm I.D.; injection time, 30 s; no experimental data for evaporation rate at various moments of injection available as no FID system was installed at end of RG. Set-up 3: 3.95 m×0.53 mm I.D. RG connected to a T-splitter via a 0.54 m×0.05 mm I.D. capillary to the FID and a 0.47 m×0.32 mm I.D. RG; injection time, 30 s.

[b] From FID response.

[c] Calculated with computer programme of Table 1.

[d] Evaporation rate at 0.05 min after start of injection.

[e] Calculated by dividing injected volume by evaporation time; value which can easily be measured in practice (correction for dead time is necessary).

I.D. retention gap, the evaporation rate increases only 12 and 3 μl/min, respectively (1 and 3 μl/min calculated). This increase is significantly lower than with the injections into a 0.32 mm I.D. retention gap described above, although more solvent is left in the retention gap after the injection is complete. After the injection, the evaporation rate increases more than during the injection, viz. 22 and 59 μl/min (calculated: 13 and 43 μl/min) for the 230- and 320-μl/min injections, respectively. This is, again, less than for the injections into the 0.32 mm I.D. retention gap of set-up 1 of Table 2.

To sum up, the differences between experimental and calculated evaporation rates at different moments during injection are less than 10% (Table 2). [Of course, the per cent differences between the experimental and calculated increases of the evaporation rate, which are obtained by subtraction, are considerably larger.] The differences between the experimental and calculated values can be attributed to assumptions made with regard to Eqs. (II) and (III) and to the solvent film distribution, to contributions of the dynamics of solvent film formation, e.g. the formation of waves [9], and the imprecision of the numerical values used for calculation. With regard to the last aspect, the examples included in Table 3 indicate that imprecisions in the evaporation rate of 1–6% can be expected as a result of the imprecision of individual parameters. The internal diameters of the retention gap and retaining precolumn, the length of the retaining precolumn, the outlet pressure and, especially, the head pressure appear to be most critical in this respect. Calculating the viscosity of the gas mixture may result in some imprecision; using Reichenberg's method rather than Wilke's as approximation results in a 4% higher evaporation rate.

In conclusion, the calculated values agree rather well with the experimental values, and the present model can be used for the (semi-quantitative) description of the change in the evaporation rate occurring during injection and evaporation. This

Table 3
Influence of imprecision of parameters on calculated evaporation rate and helium flow-rate[a]

Parameter	Value taken	Uncertainty[b]	Per cent change of	
			Evaporation rate	Helium flow-rate
Internal diameter of retention gap (mm)	0.53	0.01	−4.3	−4.4
Length of retention gap (m)	3.95	0.10	1.4	1.3
Internal diameter of retaining precolumn (mm)	0.32	0.01	−6.0	−5.7
Length of retaining precolumn (m)	0.48	0.05	5.3	6.0
Solvent film thickness (μm)	22	2	0.7	1.5
Solvent film length (m)	2.0	0.2	0.9	−2.6
Head pressure[c] (kPa)	38.7	5.0	−11	−22
		1.0	−2.2	−4.7
Column temperature (°C)	77.0	0.4	0.9	4.0
Approximate viscosity of mixture (μP)	93.5	4.3[d]	4.0	4.0
Outlet pressure (kPa)	101.3	2.0[e]	4.4	5.0

[a] Set-up 3 of Table 2; injection speed, 320 μl/min. Change of evaporation rate and helium flow calculated with computer programme of Table 1 for situation 0.04 min after start of injection.
[b] Expected uncertainty of 'value taken'; for calculation of per cent changes, uncertainty was given negative sign.
[c] Uncertainty of reading manual manometer found to be about 5 kPa.
[d] Difference of viscosity obtained when using Reichenberg's rather than Wilke's method for calculation [17].
[e] Typical maximum variation of atmospheric pressure in North-Western Europe in one month [19].

knowledge can, in its turn, be used to find the best strategy to optimize injection conditions in actual practice and to evaluate its robustness.

3.4. Optimization of PCSE on-column injection conditions

As discussed in Section 1, optimization of the injection conditions of PCSE on-column injections with, in principle, a series of injections of pure solvent can be achieved by (1) determining the evaporation rate (method A1, A2 or B) and subsequently selecting an appropriate injection speed with Eq. (I) or (2) adjusting the evaporation rate to the injection speed by varying the injection temperature (method C). However, as we now know, the change of the evaporation rate during injection and, especially, during subsequent evaporation has to be considered. The various strategies will be compared especially with regard to the latter effect. In all cases the end of evaporation was detected by means of the SVE controller.

As outlined above, one has to consider that the introduction of the injection needle may decrease the gas flow and, therefore, the evaporation rate. This is especially the case when a rather thick injection needle, as e.g. with an autosampler, is used. Therefore, during optimization, the injection syringe was left in the injector until the end of the evaporation process (in practice, the syringe was kept in the injector for 1 min after injection), because otherwise a 'mixture' of the evaporation rates with the needle inserted and withdrawn would be measured, while for the calculation of the appropriate injection speed the evaporation rate with the needle in the injector is required. For the development of the optimization strategies it was assumed that the capacity of the retention gap used was at least 20% of the injection volume.

3.4.1. Determination of evaporation rate to select appropriate injection speed (methods A–B)

For the same set-up, identical evaporation rates should be obtained with methods A1, A2 and B, if the evaporation rate were constant during injection and evaporation. However, the experimental value

Table 4
Evaporation rate by variation of injection speed or injection time (calculated values in italics)

Set-up[a]			Evaporation rate, experimental or calculated by							
No.	I.D. RG (mm)	P (kPa)	Method A1 Evap. rate (μl/min)	Method A2			Method B			
				Injection speed (μl/min)	Solvent at end of injection[b] (μl)	Evap. rate (μl/min)	Injection sped (μl/min)	Solvent at end of injection (μl)	Injection time (s)	Evap. rate (μl/min)
1	0.32	132	73 *75*	80–100	*5–23*	106 *100*	100	*5–12*	10–30	76 *77*
				100–120	*23–41*	140 *125*		*16–23*	40–60	86 *83*
3	0.53	38.7	175 *187*	200–260	*6–37*	195 *202*	240	*10–26*	10–30	179 *190*
				260–320	*37–67*	209 *221*		*36–51*	40–60	190 *200*

[a] See footnote (a) of Table 2.
[b] Calculated using the computer programme of Table 1.

determined by method A1 was significantly lower than those obtained by methods A2 and B (Table 4), and the latter two also depended on the injection speed. This was not unexpected after the above discussion, because there is not one 'true' evaporation rate, as it keeps changing during injection. A tentative explanation is as follows.

The evaporation rate determined by method A1, which is equal to the injection speed at which the time of evaporation starts to exceed the injection time (Fig. 5), is identical with the evaporation rate at the start of the injection when there is, as yet, no significant solvent film present in the retention gap. When increasing the injection speed above the evaporation rate at a constant injection time, most of the additional volume injected is deposited in the retention gap. This results in an increase of the evaporation rate during, but especially, after the injection, so that the remaining additional solvent evaporates at a higher evaporation rate. Because of this, the use of method A2 will result in a value for the evaporation rate (which is equal to the inverse of the slope of the high-injection speed part of the evaporation time vs. injection volume plot expressed as Δ evaporation time/Δ injection volume; see Fig. 5) which is larger than the evaporation rate during injection. The more solvent is left at the end of the injection (that is, the higher the injection speed is), the larger is the increase of the evaporation rate. This is reflected by the decrease of the slope of the high-injection speed part of the evaporation time vs. injection volume plot of Fig. 5. In other words, the experimentally determined value depends on the range of injection speeds chosen. With method B (see Fig. 6), a significantly larger amount of the additional volume injected during the increased injection time evaporates during injection than with method A2. Since the evaporation rate increases much less during, than after, injection, the evaporation time per injected solvent volume for the additional volume injected does not decrease as much as with method A2. Consequently, the experimentally determined value for the evaporation rate does not depend on the injection speed as much as for method A2, and will be closer to that of method A1 than of method A2.

Relevant experimental data from Table 4 can be quoted in order to illustrate the above explanation. For injection conditions which leave similar amounts of solvent in the retention gap at the end of the injection, the evaporation rates determined with method B vary less than those obtained with method A2: as the data of set-up 1 of Table 4 show, with method A2 values of 106 μl/min (5–23 μl solvent left at end of injection in retention gap) and 140 μl/min (23–41 μl solvent left) were obtained as against 76 μl/min (for injection times of 10–30 s leaving 5–12 μl in the retention gap) and 86 μl/min (for injection times 40–60 s leaving 16–23 μl) for

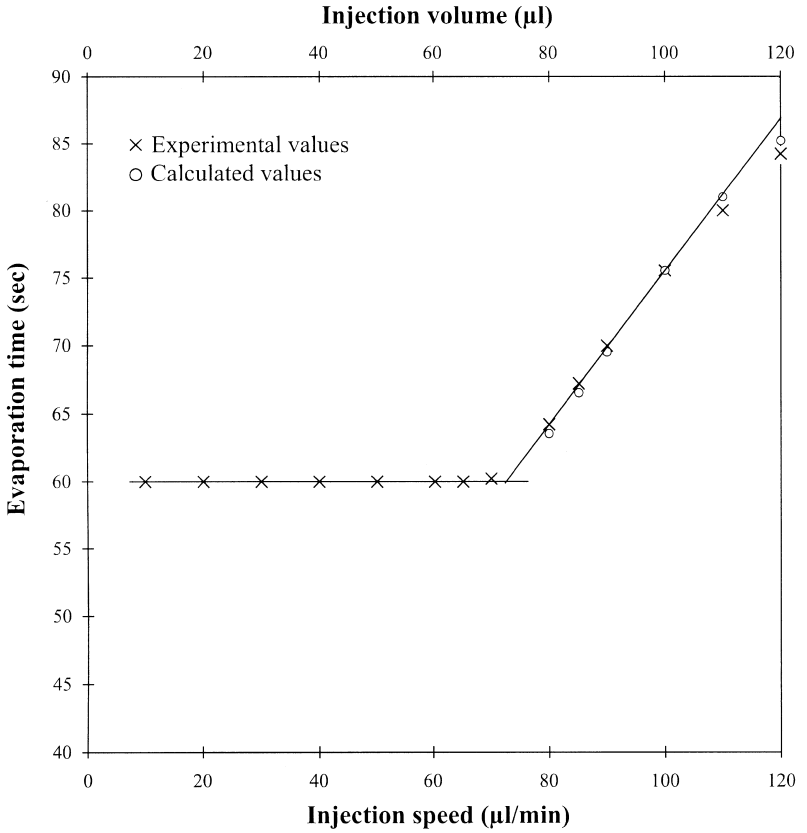

Fig. 5. (×) Experimental and (○) calculated (with programme of Table 1) evaporation times for 1-min injections performed at various injection speeds to determine the evaporation rate according to methods A1 and A2 (for details, see text). Slope of the high-injection speed plot obtained by linear regression of experimental data obtained at 80–100 µl/min injection speeds. Injection was done via a 0.25 mm O.D needle into a 5.95 m×0.32 mm I.D. retention gap of the set-up of Fig. 3. The injection needle was not removed after the injection.

method B. The value of 73 µl/min obtained with method A1 (which is identical to the evaporation rate at the start of the injection) is below the mean evaporation rate during the injection and evaporation (77 µl/min for a 90-µl/min injection and 86 µl/min for a 120-µl/min injection; cf. Table 2). The values obtained with method B (76 and 86 µl/min) are below the evaporation rate at the end of the evaporation (89 µl/min for a 90-µl/min injection and 105 µl/min for a 120-µl/min injection; cf. Table 2) and are closely similar to the mean evaporation rates. The values obtained with method A2 are, on the other hand, significantly higher than the mean evaporation rates, and actually, can even exceed the evaporation rate at the end of the evaporation!

In all instances do the experimental data agree well with the data calculated with the programme of Table 1 (see Table 4 and Figs. 5 and 6). The mutual differences of less than 10% demonstrate the good agreement between theory and experiment. It can be added that a similar trend was found for the determination of the evaporation rate for injections into a 0.53 mm I.D. retention gaps (Table 4, set-up 3), with the mutual differences being somewhat smaller than for the 0.32 mm I.D. retention gap.

Obviously, when trying to select an appropriate injection speed, method A2 cannot be recommended to determine the evaporation rate: overestimation of the mean evaporation rate will easily occur, which can result in choosing an injection speed at which flooding of the retaining precolumn may occur. This can, e.g., be the case when using the experimentally

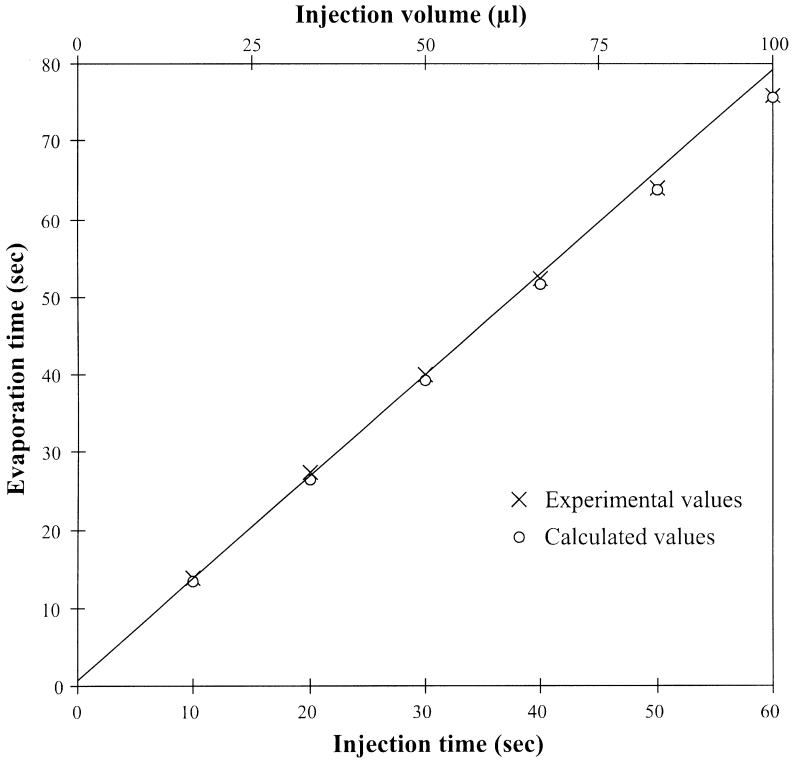

Fig. 6. (×) Experimental and (○) calculated (with programme of Table 1) evaporation time for 100-µl/min injections performed during various injection times to determine the evaporation rate of ethyl acetate by means of method B (for details, see text). Slope obtained by linear regression of experimental data obtained for 10–30 s injection times. Evaporation time does not increase exactly linearly with injection volume; therefore, measurements should be made such that evaporation time does not exceed injection time more than 30–40%. Injection was done via a 0.25 mm O.D needle into 5.95 m×0.32 mm I.D. retention gap of the set-up 1 of Table 2. The injection needle was not removed after the injection.

determined value of the evaporation rate of 140 µl/min (Table 4, set-up 1) for the selection of the appropriate injection speed from Eq. (I): for a 200-µl injection and $f=0.60$, an injection speed of 173 µl/min is then calculated. However, as the calculation programme of Table 1 readily shows, with this injection speed the length of the solvent film will exceed the length of the retention gap just after completion of injection, i.e. when the solvent film is pushed further into the retention gap during its evaporation. For practical reasons, we prefer method B over method A1, because a smaller number of injections of pure solvent is required-typically, 3–4 against 5–8, according to our experience.

Finally, as regards the calculation of an appropriate injection speed from Eq. (I), a compromise has to be made to assure that a solvent film of sufficient (but not excessive; see above) length is formed to retain the volatile analytes and there has to be a safety range to compensate for small changes of, e.g., the injection volume during a series of analyses and differences between the calculated and experimentally solvent film length (see Section 3.4.2.). Therefore, we generally prefer $f=0.6$ to calculate the appropriate injection speed.

3.4.2. Adjusting the evaporation rate to the injection speed (method C)

As discussed above, method B is recommended for the optimization of the injection conditions of a new set-up or when using a new solvent for injection. However, if only slight changes have to be made, such as after the exchange of the retention gap, and the optimal injection conditions are there-

fore rather well known, the simpler method C (see Section 1.2.) can be used. Here, the evaporation rate is varied by varying the injection temperature at a fixed injection speed and head pressure to adjust the evaporation rate to the injection speed until the targeted value of ϑ = injection time/evaporation time is obtained. Optimization is started with the injection temperature used prior to the minor modification of the system (and with the injection volume selected for the subsequent, or on-going, real-life analyses).

Similarly to what was said above about the desired value of f (method B), in the case of selecting a proper value of ϑ, one has to consider that the solvent film in the retention gap should be of sufficient length, but should not exceed the length of the retention gap. When taking small experimental changes and possible differences of calculated and experimental values of ϑ into account, according to our experience it is advisable to select the value of ϑ such that $f=0.5$ (for both 0.32 and 0.53 mm I.D. retention gaps), or, in other words, that half of the capacity of the retention gap is used.

To illustrate the above, a 100-μl injection of ethyl acetate into a 5.65 m×0.32 mm I.D. retention gap with a capacity of about 60 μl is considered. For $f=0.5$, 70% of the solvent has to be evaporated during injection or, in other words, the targeted value of ϑ should be 0.7. As a demonstration of the variation of ϑ with the (injection) temperature, Table 5 lists values for temperatures from 88°C down to 72°C. As is to be expected, a decrease of the injection temperature results in a decrease of ϑ. The mutual differences of less than 10% between the experimental values and the values calculated with the programme of Table 1 demonstrate the good agreement between theory and experiment. Values such as are shown in Table 5 are, strictly speaking, of course valid for one set-up ('the present retention gap and press-fit') only. Experience shows that the difference in the injection temperatures at which the targeted ϑ value was obtained prior to, and after, the exchange of a retention gap, was only ±(0–1)°C.

Finally, it is interesting to emphasize that $100\cdot\vartheta$ is not exactly equal to the percentage of solvent evaporated during injection – which it would be if the evaporation rate were constant – but is somewhat higher, as is obvious from the data of Table 5. That is, more solvent is left in the retention gap after the injection than is suggested by ϑ. This can be attributed to the increase of the evaporation rate after the injection: a higher percentage of solvent evaporates after the injection than is suggested by the experimental value of ϑ, which reflects the average evaporation rate/injection rate ratio. To quote an example obtained by using the calculation programme of Table 1, for a 100-μl injection at 76°C, $\vartheta=0.77$, but only 74% of the solvent evaporates during the injection. Screening of the data in the

Table 5
Optimization of injection temperature for ethyl acetate by adjusting evaporation rate[a]

Injection temperature (°C)	Ratio ϑ[b]		Calculated[c] per cent solvent evaporated during injection
	Experimental	Calculated[c]	
88	1.00	1.00	100
86	0.98	1.00	100
84	0.95	1.00	100
82	0.89	0.94	94
80	0.85	0.88	87
78	0.81	0.82	80
76	0.77	0.77	74
74	0.73	0.72	69
72	0.70	0.68	63

[a] Set-up no. 1 of Table 2; 100-μl injections at 100 μl/min; head pressure, 132 kPa He. Injection needle left in injector after injection for further 60 s.

[b] ϑ (=injection time/evaporation time) equals fraction of solvent evaporated during injection if evaporation rate should be constant during injection and evaporation. Evaporation time determined by SVE controller (time of closure of SVE).

[c] Using the programme of Table 1. Simple experimental determination of percentage of solvent evaporated during injection is not possible.

Table shows that, in order to be on the safe side, one has to assume that up to 5% more solvent may be left in the retention gap than is suggested by ϑ if 65–85% solvent evaporation during injection. This is actually the reason for choosing ϑ such that $f=0.5$ (and $f=0.6$ in Section 3.4.1.), because then solvent film lengths of 55–70% of the total length of the retention gap are predicted by the calculation programme of Table 1.

It is interesting to add that, if the injection speed can be chosen only in rather large steps – e.g. with the AS 800 autosampler injections speeds of only 1, 2, 3 etc. μl/s can be chosen – selecting an appropriate injection speed after determination of the evaporation rate is not possible. In this case, method C is also preferred when the optimal injection conditions are not known. The temperature at which optimization is started should then be just below the boiling point of the solvent at the selected head pressure and some 4–8 injections are required.

3.5. Analysis of aqueous samples by LLE–LVI-GC–MS

The potential of the present LVI-GC approach was demonstrated for the analysis of aqueous samples using mass-selective detection. The use of LVI-GC allows the miniaturization and simplification of sample preparation by in-vial LLE: 0.16 mg sodium chloride was weighed into a 2-ml vial, a 0.8-ml aqueous sample and 0.8 ml of *n*-hexane were added and mixed by shaking for 2 min and placed in the autosampler tray for analysis. Next, 100 μl of the organic extract were injected into the GC–MS system. The SVE was automatically closed by the SVE controller, and the injection conditions were optimized by means of method C using an injection speed of 120 μl/min and $\vartheta=0.7$. Actually, after exchange of the retention gap, a maximum of only two injections were required to find the injection temperature resulting in the targeted value of ϑ, which was in most cases 70°C.

The aim was the determination of analytes as volatile as monochlorobenzene. Recently, we demonstrated that the determination of monochlorobenzene is not possible with conventional on-line solid-phase extraction (SPE)–GC. This was attributed to the non-uniform distribution of the analytes in the solvent film during an on-line SPE–GC transfer, i.e. to the fact that the major part of the analytes is deposited in the front part of the solvent film [18]. Quantitative recovery of monochlorobenzene could be achieved only if a so-called presolvent was introduced prior to desorption.

A preliminary series of injections of a 100-μl injection of the test mixture in *n*-hexane showed that the recoveries of all analytes – i.e., also of the more volatile compounds – were at least 80% compared with a standard 1-μl injection. This demonstrated that the present optimization strategy and the use of a controller for the closure of the SVE indeed allows the determination of volatile analytes. As regards the results of the total procedure, the recoveries were very good (85–110%) for 50 out of the 52 test compounds (Table 6). Somewhat lower recoveries were obtained only for compound Nos. 36 (82%) and 29 (65%). This can be attributed to their rather polar nature, which is reflected by their low octanol–water coefficients (K_{OW}): their log K_{OW} values are 1.2 and 0.8, respectively. The relative standard deviation of the recovery data was found to be satisfactory for all test compounds (1–9%; $n=6$). Fig. 7 shows the total ion chromatogram of the LLE–LVI-GC–MS analysis of 0.8-ml HPLC-grade sample spiked with 10 μg/L of the test analytes. The detection limits using the reconstructed ion chromatograms were typically 20–250 ng/l. The analysis of real matrices like tap and river water will be the topic of our next paper.

4. Conclusions

Recent studies indicate that monitoring of the helium flow-rate is a simple and reliable method to control large-volume on-column injections in GC. Closure of SVE at the very end of evaporation increases the capacity of the retention gap. This is readily (and automatically) achieved by means of the SVE controller, while closing at a pre-determined value at the very end can result in loss of volatiles when the evaporation time slightly shifts, e.g., due to small changes in the injection volume.

Experiments show, and theory can explain, that the evaporation rate changes during injection and,

Table 6
Recovery of micropollutants after LLE–LVI-GC–MS of 0.8-ml HPLC-grade water spiked at the 10-μg/l level

No.	Compound	Recovery[a] (%)	No.	Compound	Recovery[a] (%)
1	Monochlorobenzene	102	27	Nitrobenzene	100
2	Chlorohexane	111	28	*N*,*N*-Dimethylphenol	97
3	Ethylbenzene	106	29	Triethyl phosphate	65
4	*p*/*m*-Dimethylbenzene	97	30	*N*-Ethylaniline	101
5	Styrene	100	31	Isoforon	100
6	*o*-Dimethylbenzene	100	32	1,3,5-Trichlorobenzene	101
7	Methoxybenzene	101	33	1,4-Dimethoxybenzene	101
8	1,2,3-Trichloropropane	100	34	2,4+2,6-Dimethylaniline	98
9	Propylbenzene	101	35	2,4-Dichlorophenol	88
10	*o*-Chlorotoluene	99	36	2-Methoxyaniline	82
11	Benzaldehyde	99	37	1,2,4-Trichlorobenzene	102
12	1,2,3-Trimethyl thiophosphate	96	38	Naphthalene	104
13	2,4,6-Trimethylpyridine	96	39	Hexachlorobutadiene	102
14	Benzonitrile	94	40	1,2,3-Trichlorobenzene	102
15	*m*-Dichlorobenzene	101	41	α,α,α-Trichlorotoluene	107
16	*p*-Dichlorobenzene	96	42	1-Chlorodecane	99
17	5-Ethyl-2-methylpyridine	121	43	Quinoline	108
18	Indane	103	44	1-Chloro-4-nitrobenzene	101
19	*o*-Dichlorobenzene	100	45	1-Chloro-2-nitrobenzene	102
20	Indene	102	46	Isoquinoline	96
21	Butylbenzene	97	47	1H-Indole	91
22	*N*-Methylaniline	85	48	1,4-Diethoxybenzene	93
23	2-Methylphenol	97	49	1-Methylnaphthalene	105
24	2-Methylbenzeneamine	101	50	Ferrocene	102
25	Acetophenone	92	51	2-Methylisoquinoline	100
26	*N*,*N*-Dimethylamine	100	52	1,2,4,5-Tetrachlorobenzene	101

[a] 4, 4′-Difluorobiphenyl used as internal standard. Recoveries calculated using a 100-μl standard injection as reference.

even more so, during subsequent evaporation, and that this change is more significant for injections into a 0.32 mm I.D., than into a 0.53 mm I.D. retention gap. This effect significantly influences the optimization of injection conditions of PCSE on-column injections. A comparison of four methods which are commonly used to determine the proper injection conditions showed that two of these can be recommended for practical work:

- determination of the evaporation rate by increasing the injection time at a constant injection speed and subsequent calculation of an appropriate injection speed from Eq. (I) (method B) is preferred when the optimal conditions are essentially unknown;
- if re-optimization of an on-column injection after, e.g., exchange of the retention gap, is required and the optimal conditions are known fairly well, adjusting of the evaporation rate to the injection speed by variation of the injection temperature at a constant injection speed (method C) is preferred.

Although the experimentally determined values of the amount of solvent evaporated during injection and evaporation (ϑ, method C), or the length of the solvent film in the retention gap (f, method B, no data shown) may differ somewhat from the targeted values due to the change of the evaporation rate during injection and evaporation, both methods can be used without any risk of flooding or losing volatile analytes if the injection conditions are calculated from the experimental values as described above. With both strategies, optimization of the injection speed is straightforward and rapid: two (method C) to five (method B) injections of pure solvent are required without any reconstruction of the set-up. A logical next step seems to be the development of appropriate software which will

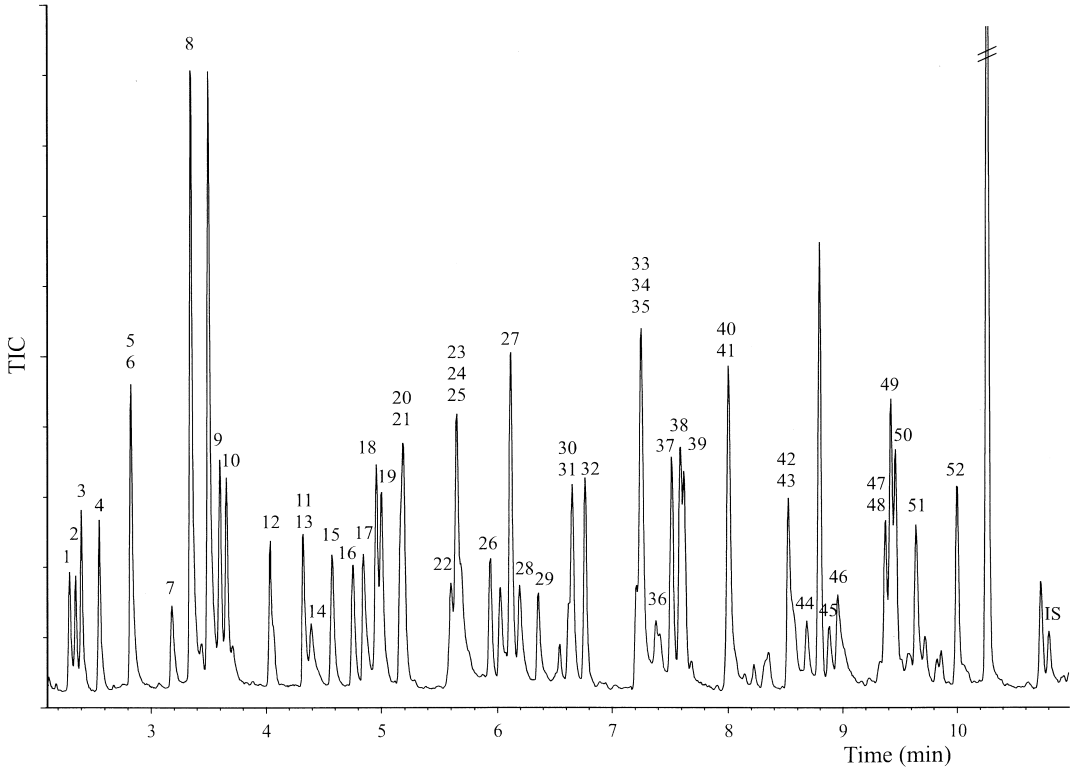

Fig. 7. Total ion current LLE–LVI-GC–full-scan MS of a 0.8-ml water sample spiked with 52 micropollutants at the 10-μg/l level. For peak assignment, see Table 6. Unknown compounds are co-eluting with analytes nos. 8 and 27.

enable automated system optimization without the assistance of an operator.

Acknowledgements

The authors thank the European Union for their support to Th. Hankemeier via a Human Capital and Mobility grant (No. EV5V-CT-93-5225).

References

[1] Th. Hankemeier, H.T.C. van der Laan, J.J. Vreuls, M.J. Vredenbregt, T. Visser, U.A.Th. Brinkman, J. Chromatogr. A 732 (1996) 75.
[2] F.D. Rinkema, A.J.H. Louter, U.A.Th. Brinkman, J. Chromatogr. A 678 (1994) 289.
[3] H.-J. Stan, M. Linkerhägner, J. Chromatogr. A 727 (1996) 275.
[4] H.G.J. Mol, H.-G.M. Janssen, C.A. Cramers, J.J. Vreuls, U.A.Th. Brinkman, J. Chromatogr. A 703 (1995) 277.
[5] A. Venema, J.T. Jelink, J. High Resolut. Chromatogr. 19 (1996) 234.
[6] K. Grob, H.-G. Schmarr, A. Mosandl, J. High Resolut. Chromatogr. 12 (1989) 375.
[7] F. Munari, A. Trisciani, G. Mapelli, S. Trestianu, K. Grob, J.M. Colin, J. High Resolut. Chromatogr. Chromatogr. Commun. 8 (1985) 601.
[8] K. Grob Jr., G. Karrer, M.-L. Riekkola, J. Chromatogr. 334 (1985) 129.
[9] K. Grob, in: W. Bertsch, W.G. Jennings, P. Sandra (Eds.), On-line Coupled LC–GC, Hüthig, Heidelberg, 1991.
[10] S. Ramalho, Th. Hankemeier, M. de Jong, U.A.Th. Brinkman, J.J. Vreuls, J. Microcol. Sep. 7 (1995) 383.
[11] Th. Hankemeier, S.J. Kok, J.J. Vreuls, U.A.Th. Brinkman, J. Chromatogr. A 811 (1998) 105.
[12] E. Boselli, B. Grolimund, K. Grob, G. Lercker, R. Amadò, J. High Resolut. Chromatogr. 21 (1998) 355.
[13] J. Staniewski and K. Alejski, poster presented at the 18th International Symposium on Capillary Chromatography, Riva del Garda, 1996.
[14] J.J. Vreuls, G.J. de Jong, R.T. Ghijsen, U.A.Th. Brinkman, J. Ass. Off. Anal. Chem 77 (1994) 306.

[15] Th. Hankemeier, A.J.G. Mank, J.J. Vreuls, U.A.Th. Brinkman, in preparation.
[16] J.J. Vreuls, W.J.G.M. Cuppen, G.J. de Jong, U.A.Th. Brinkman, J. High Resolut. Chromatogr. 13 (1990) 157.
[17] R.C. Reid, J.M. Prausnitz, B.E. Poling, The Properties of Gases and Liquids, 4th ed, McGraw-Hill, New York, 1987.
[18] Th. Hankemeier, S.P.J. van Leeuwen, J.J. Vreuls, U.A.Th. Brinkman, J. Chromatogr. A 811 (1998) 117.
[19] Data from WWW site of Institute for Meterology of Free University Berlin; Internet: http://user.cs.tu-berlin.de/~eserte/met/wetter-1998.